

## SURVEY AND SUMMARY

# The impact of recent improvements in cryo-electron microscopy technology on the understanding of bacterial ribosome assembly

Aida Razi<sup>1</sup>, Robert A. Britton<sup>2</sup> and Joaquin Ortega<sup>1,\*</sup>

<sup>1</sup>Department of Biochemistry and Biomedical Sciences and M. G. DeGroote Institute for Infectious Diseases Research, McMaster University, Hamilton, Ontario L8S 4K1, Canada and <sup>2</sup>Department of Molecular Virology and Microbiology and Center for Metagenomics and Microbiome Research, Baylor College of Medicine, Houston, TX 77030, USA

Received August 30, 2016; Revised November 20, 2016; Editorial Decision November 22, 2016; Accepted November 25, 2016

### ABSTRACT

Cryo-electron microscopy (cryo-EM) had played a central role in the study of ribosome structure and the process of translation in bacteria since the development of this technique in the mid 1980s. Until recently cryo-EM structures were limited to ~10 Å in the best cases. However, the recent advent of direct electron detectors has greatly improved the resolution of cryo-EM structures to the point where atomic resolution is now achievable. This improved resolution will allow cryo-EM to make groundbreaking contributions in essential aspects of ribosome biology, including the assembly process. In this review, we summarize important insights that cryo-EM, in combination with chemical and genetic approaches, has already brought to our current understanding of the ribosomal assembly process in bacteria using previous detector technology. More importantly, we discuss how the higher resolution structures now attainable with direct electron detectors can be leveraged to propose precise testable models regarding this process. These structures will provide an effective platform to develop new antibiotics that target this fundamental cellular process.

### INTRODUCTION

X-ray crystallography and cryo-electron microscopy (cryo-EM) have been key techniques used to understand the structure and function of the bacterial ribosome. In the year 2000, the groups of Venki Ramakrishnan, Tom Steitz and

Ada Yonath published atomic resolution structures of the 30S and 50S ribosomal subunits (1–3). This historical landmark culminated a long quest aimed at solving the structure of the ribosome that started in the 1970s in Harry Noller's laboratory when the secondary structure of the 16S and 23S rRNA was elucidated. In the time span between these two historical landmarks, many groups contributed to slowly define the topography of the bacterial ribosome. To name a few, significant progress was obtained by the Stöfler's group (4,5) using immune electron microscopy to define the spatial arrangement of the ribosomal proteins (r-proteins). Cross-linking approaches in the Brimacombe's group (6–8) allowed to reveal r-protein-rRNA and r-protein contacts. Peter Moore and Don Engelman used neutron scattering to determine the relative positions of the r-proteins in the 30S subunit (9) and comparative sequence analysis was also instrumental to infer the higher order structures adopted by the 5S, 16S and 23S rRNAs (10–15).

All along, but especially after the development of the specimen vitrification process by Dubochet *et al.* (16) in 1984, cryo-EM has contributed significantly to the joint effort of determining the structure of the ribosome. Initially, low-resolution cryo-EM maps of the ribosome, mainly from Frank's group (17), provided the envelopes to dock high-resolution structures of individual r-proteins and fragments of RNA that several groups were busy solving. Around the 1990s, it was believed that this divide and conquer approach would eventually render the atomic resolution structure of the 70S ribosome (18). However, in the latter half for the 1990s solid progress in ribosome crystallization and concurrent improvements in synchrotron radiation sources led to the structural determination of ribosomal subunits at atomic resolution from entire particles.

\*To whom correspondence should be addressed. Tel: +1 905 525 9140 (Ext 22703); Fax: +1 905 522 9033; Email: ortega@mcmaster.ca

The contributions of cryo-EM to ribosome biology are not only limited to structure. An important part of our understanding of the protein synthesis process is also derived from cryo-EM. An important challenge in this effort has always been that the ribosome is a molecule in constant motion and that fluctuates between different states during the process of protein translation (19–21). Most of these states constitute transient structures that are difficult to trap in a crystalline form, and consequently challenging to be solved by X-ray crystallography. However, mixtures of complexes populating the ribosome work cycle and coexisting in the same sample are not a limiting factor for cryo-EM. Image classification approaches (22–25) have long been used to separate particle subpopulations and build 3D reconstructions for each conformer in the mixture.

Until recently, the drawback of this approach was that the resolution of the resulting reconstructions was limited to  $\sim 8 \text{ \AA}$  resolution in the best cases (26,27). Atomic resolution models were only attainable when all the individual components of the complex were known to atomic resolution and it was possible to dock them unambiguously into the limited resolution cryo-EM maps (28). Recent advances in direct electron detector cameras (direct detectors) have dramatically changed the resolution limit that is now attainable by cryo-EM (29–31). These detectors have opened a much easier way to gather atomic resolution information on translating ribosome intermediates that are extremely challenging to crystallize. The avalanche of ribosome structures in the 3–4  $\text{\AA}$  resolution range that have recently been produced from these new detectors (32–36) demonstrate that it is currently possible to retrieve the entire inventory of states co-existing during the work cycle of the ribosome and gain a complete portrait of the protein synthesis process in three dimensions.

These recently published structures of mature ribosomes provide little insight into ribosome biogenesis. The next frontier in the ribosome field is to understand the assembly process. Ribosomal subunit assembly has been the subject of >50 years of investigation that began with seminal studies by the Nomura (37–41) and Nierhaus (42–44) laboratories in the late 1960s and early 1970s to map the reconstitution of the 30S and 50S subunits *in vitro*. Structural interest in this field has resurfaced in the last several years, sparked by the publication of several cryo-EM structures of ribosome assembly intermediates (Figure 1A) (45–51) and complexes of ribosomal subunits with protein assembly factors (Figure 1B) (52–55). All these structures were produced from electron micrographs collected either on photographic film or standard charge-couple device (CCD) cameras. Consequently, the obtained resolution in these structures was  $\sim 10 \text{ \AA}$  or lower. The advent of direct electron detectors now offers the possibility to study these assembly intermediates and complexes at atomic resolution, which will most likely transform our understanding of the ribosome assembly process.

In this review, we briefly describe how in light of recent progress in direct electron detector devices, cryo-EM represents now an ideal tool to study the process of assembly of the ribosome. We also summarize the main contributions that cryo-EM so far has brought in combination with chemical and genetic approaches to our understanding of this

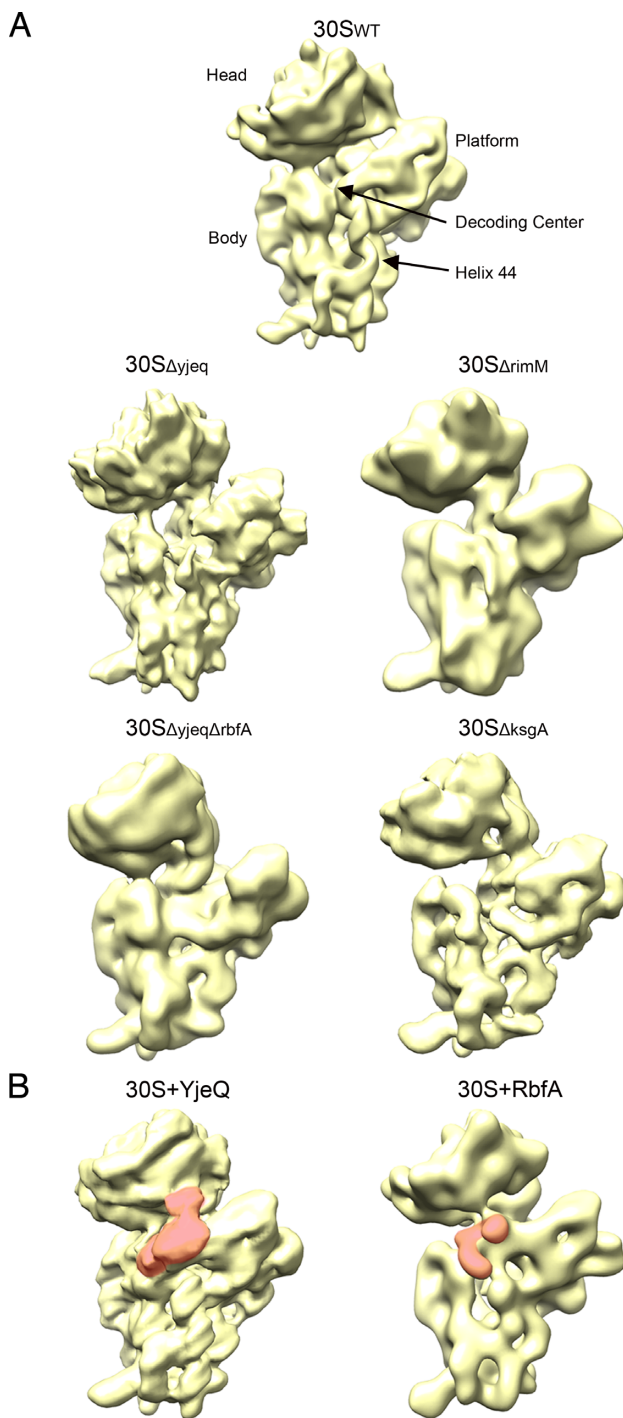


**Figure 1.** Cryo-EM structure of 30S subunit assembly intermediates and complexes of the 30S subunit with assembly factors. **(A)** Gallery of cryo-EM structures of immature 30S subunit that accumulate in *Escherichia coli* strains lacking one or multiple assembly factors. The assembly factor that has been knocked out in the strain is indicated in the label. A density map of the mature 30S subunit is at the top of the panel for comparison purposes. This structure was obtained by applying a 20  $\text{\AA}$  low pass filter to the atomic structure of the 30S subunit (PDB ID: 2AVY). All these structures were obtained at resolutions ranging from 11 to 17  $\text{\AA}$  resolution and from images recorded on a CCD camera or film. **(B)** Cryo-EM structures of the 30S subunit in complex with either YjeQ or RbfA. These structures were obtained at 10 and 12  $\text{\AA}$  resolution, respectively. Images for the 30S + YjeQ complex were recorded in a CCD camera and the images for the complex with RbfA were recorded on film.

process in bacteria. Finally, we discuss the potential that the new direct electron detectors will provide into how ribosome assembly occurs.

## OVERVIEW OF THE RIBOSOME ASSEMBLY PROCESS IN BACTERIA

The bacterial 70S ribosome is a ribonucleoprotein complex composed of a large 50S and small 30S subunit. The 30S subunit is responsible for the decoding of the mRNA and consists of the 16S rRNA molecule and 21 r-proteins named from S1 to S21 (with a u or b prefix) (56). The 50S subunit contains the active center where peptide bond formation is catalyzed and it is made of two RNA molecules, the 23S and 5S rRNAs and 34 r-proteins designated from L1 to L36 (with a u or b prefix) (56). The three rRNA molecules form the core of the particles, whereas r-proteins mainly sit on the surface of the structure.

Bacterial ribosome assembly commences with the transcription of rRNA as a single precursor transcript containing the three rRNAs for the two subunits (along with one or two tRNA molecules) (57). RNase III performs the primary processing that separates the three rRNAs. The resulting fragments are called precursor rRNAs and contain additional nucleotides at both their 5' and 3' ends called precursor sequences (57). The coordinated action of multiple RNases removes the precursor sequences to generate the mature rRNA molecules. After transcription, the rRNA molecules undergo covalent modifications and form local secondary structures that are rapidly recognized and bound by r-proteins. Vintage studies by Nomura (37,38,40,58), Nierhaus (59,60) and more recent experiments from the Williamson and Woodson laboratories (61,62) have defined the hierarchy of binding of r-proteins and the forces shaping rRNA and r-protein interactions during subunit assembly. The binding of r-proteins is designated as primary (directly to the rRNA), secondary (dependent on primary r-proteins) or tertiary (dependent on secondary r-proteins). Evidence to date suggests that r-protein binding to the rRNA drives folding that stabilizes local RNA structure and induces conformational changes to create new binding sites for secondary proteins (63,64). Likewise, these studies suggest that, at least *in vitro*, ribosome assembly appears to occur via multiple parallel pathways without significant rate-limiting steps, outlining a process of large complexity and built-in redundancy to ensure efficient assembly even under unfavorable conditions (62,65).

Mainly through genetic approaches and through the slow assembly of ribosomes *in vitro*, the field came to realize that in cells the assembly process is extremely efficient because of being assisted by many assembly factors. These factors included enzymes responsible for the processing and covalent modifications of the rRNA and ribosomal proteins, rRNA chaperones, GTPases and helicases (66–69). However, for most of the factors their precise functions in ribosome biogenesis are still uncharacterized (70).

## CRYO-ELECTRON MICROSCOPY AS AN IDEAL TOOL FOR STUDYING RIBOSOME BIOGENESIS

Similarly, to the protein translation process, all aspects of the ribosome assembly process involve dynamic events. The

assembling ribosome is a complex in constant change. New r-proteins are incorporated and its rRNA is being covalently modified and processed as it fluctuates between different conformations. The complexity and dynamics inherent to the ribosome represents a major limiting factor for the crystallization of ribosome assembly intermediates and thus, their study using X-ray crystallography (71). In cryo-EM, the assembling ribosomes are embedded in a thin layer of vitreous ice and remain in a fully hydrated state (16,72). Ribosomal particles are not forced into any crystal lattice or subjected to steric constraints, therefore, in principle cryo-EM allows for the visualization of the entire dynamic course of the assembly process. One limitation to keep in mind is that because multiple copies of assembling ribosomes that have the same structure must be averaged to produce the 3D structure, the assembly states that are more easily observed are those that represent long-lived intermediates or local minima conformations within the free-energy landscape of the ribosome assembly process.

All the existing chemical or genetic approaches presently used (see below) to capture assembly intermediates in bacteria invariably produce a heterogeneous mixture of complexes that must be sorted out. In the last decade several image-processing packages for cryo-EM images (73–75) have implemented maximum-likelihood (ML) classification approaches (22) to sort out the particle images into structurally homogeneous subsets. This methodology has been proven to be very robust for classifying noisy cryo-EM images. Once the different subpopulations have been identified and separated, individual 3D reconstructions at atomic resolution can be generated for each of the individual assembly intermediates.

Until recently cryo-EM images from the electron microscope were recorded in photographic film. Subsequently, the field transitioned to the use of CCD cameras. These cameras allowed for the development of automation during data collection and offered the possibility to produce more and significantly larger data sets that allowed for higher resolution 3D structures and to study structurally heterogeneous assemblies (76,77). However, the attenuation of the signal and blurring of the image resulting from the indirect detection of the electrons in these devices often resulted in structures that were limited to ~10–15 Å resolution (Figure 2A). The recent development of direct detectors has transformed cryo-EM into a much more powerful technique. These devices record electrons directly with little or no noise. Images collected in these detectors contain much higher contrast and have better preservation of the high-resolution signal (Figure 2B) (29,78). Images obtained in a detector are capable to produce 3D structures to much higher resolution (Figure 2B) (<3 Å in many cases) than those obtained from CCD cameras (Figure 2A). Direct detectors also have extremely fast image read-outs, which produce ‘movies’ instead of single snapshots. Movies produced by these detectors allow compensating for ‘beam-induced motion’. This is the movement that the particles in the specimen experience because of the energy deposited by the electron beam while the image is being collected, resulting in blurring and resolution degradation (79,80). Collecting multi-frame movies instead of single snapshots allows for an effective tracking and correction of this movement efficiently restoring the

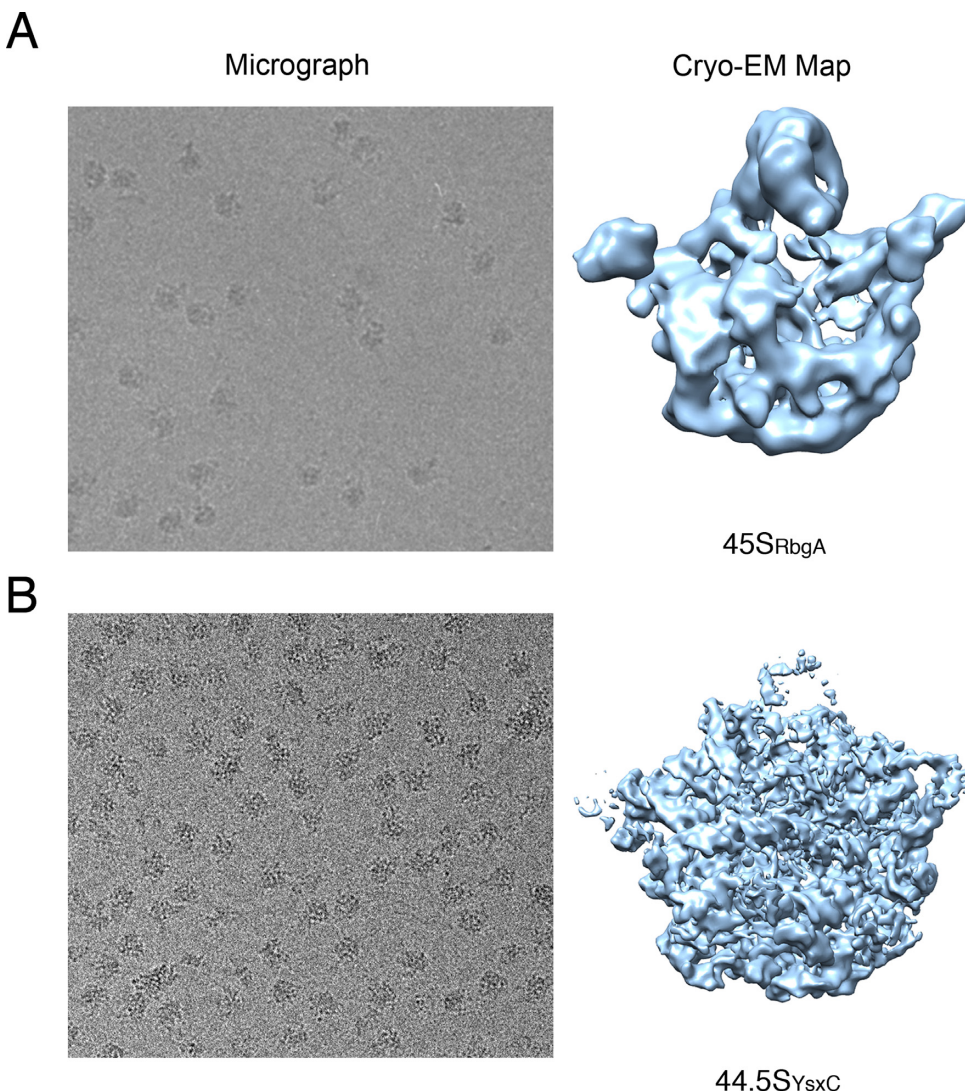


**Figure 2.** Direct detectors produce images with better preservation of the high-resolution information. (A) Cryo-electron micrograph (left panel) obtained in a CCD camera showing immature  $45S_{RbgA}$  ribosomal particles obtained from a depletion strain of *Bacillus subtilis* lacking the RbgA protein. The right panel shows a 3D reconstruction of the  $45S_{RbgA}$  particle obtained from CCD images similar to that displayed on the left panel. This 3D structure was refined to 13 Å resolution. (B) Cryo-electron micrograph (left panel) of a similar immature ribosomal particle ( $44.5S_{YsxC}$  particle) obtained in a direct electron detector. These particles were purified from a depletion strain of *B. subtilis* lacking the YsxC protein. The contrast and structural details in this image are significantly higher than in the equivalent micrograph from a CCD shown in panel (A). Direct detector images similar to that shown in this panel, produced a 3D structure at ~5 Å resolution.

high resolution in the images (30,81,82) (Figure 3). Overall, direct detectors represent a quantum leap for the capability of cryo-EM to deliver atomic resolution (27) and recently published ribosome structures (34,83–85) constitute outstanding examples of what is now possible using cryo-EM. These structures illustrate the current potential of cryo-EM to gather atomic resolution structural information of the ribosome assembly process.

Therefore, because of major improvements in both software and hardware, cryo-EM can now deliver atomic resolution structures. These advances make cryo-EM an ideal tool for the structural understanding of dynamic processes such as the assembly of the ribosome. Cryo-EM is definitively poised to bring a flood of new biological insights into this complex biological process in the upcoming years.

#### CHEMICAL AND GENETIC APPROACHES TO CAPTURE *IN VIVO* ASSEMBLED RIBOSOMAL SUBUNIT INTERMEDIATES FOR STRUCTURAL STUDIES

The Williamson lab was among the first groups to analyze bacterial immature ribosomal particles using electron microscopy (86). In this pioneer study, 30S subunits were assembled *in vitro* from purified 16S rRNA and ribosomal proteins. As the assembly reaction was allowed to proceed, aliquots were removed and imaged by negative staining electron microscopy. Using this approach, it was possible to observe many 30S particles at different stages of the maturation process. More importantly, this analysis showed that image classification approaches were effective in sorting out the multiple subpopulations of intermediates existing at the various time points without the need for biochemical pu-

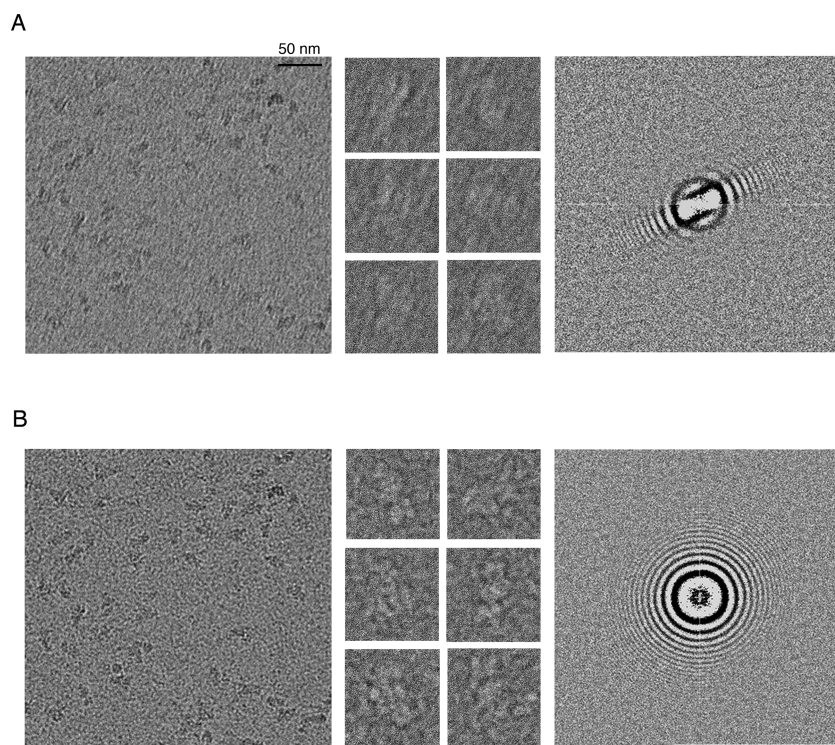


**Figure 3.** Restoration of high-resolution information by beam-induced correction. (A) Micrograph showing 30S ribosomal subunits obtained by merging the 30 frames from a movie obtained in a Gatan K2 direct electron detector without previous beam-induced motion correction. The micrograph (left) and particles (center) extracted from this micrograph are clearly drifted. The disappearance of the 'Thon rings' in the power spectra from the micrograph reveals the loss of high-resolution information due to drifting. The power spectra are obtained by calculating the Fourier Transform of the micrograph. (B) Performing beam-induced motion correction of the movie frames prior to generating the merged image recovers the high-resolution information in the micrograph (right panel). This is demonstrated by analysis of the power spectra of the corrected micrograph that shows clearly defined 'Thon rings'. Both the micrograph and extracted particles also do not show any sign of drifting after the beam-induced motion correction was applied.

Downloaded from https://academic.oup.com/nar/article/45/3/1027/2651561 by guest on 05 August 2023

rification. These results also provided specific structural evidence for the existence of parallel assembly pathways *in vitro*. However, the question remaining was whether the observed structures recapitulate the assembly intermediates existing *in vivo*.

A significant challenge faced to structurally study the ribosome assembly process *in vivo* is that bacteria are highly efficient in assembling ribosomes and the process occurs in a timescale of just a few minutes. Consequently, ribosome assembly intermediates do not naturally accumulate in significant amounts in bacterial cells (87). To date, structural biologists have leveraged mainly two types of approaches to trigger accumulation of assembly intermediates: chemical and genetic.

The essence of the chemical approach consists of using a small-molecule inhibitor to disable or slow down a specific step in the ribosome assembly process, leading to the accumulation of immature subunits that can be purified and characterized (Figure 4A). Using small-molecule inhibitors as probes for studying a complex biological process has advantages. For example, the chemical compound can be added or removed easily from the cell system and the inhibition effect appears in a time scale of minutes (88).

This type of approach was instrumental in the dissection of the protein synthesis process. This was possible because there is a plethora of chemical probes (antibiotics and other small molecule inhibitors) that affect this process (89,90)

and they were used extensively to capture ribosomes in numerous conformational states during protein translation.

Unfortunately, presently there is a scarcity of chemical probes that could be used to study the assembly process of the ribosome. Some of the antibiotics inhibiting translation cause accumulation of 30S and 50S ribosomal subunit precursors (91). However, to date, only lamotrigine, a drug that is also used as an anticonvulsant, has been confirmed as a specific inhibitor of bacterial ribosome biogenesis by targeting a still uncharacterized function of the translation initiation factor IF2 in ribosome assembly. This effect only takes place at cold temperatures but not at 37°C (92). In eukaryotes, only three other compounds have been shown to inhibit specific factors in ribosome assembly in eukaryotes (93–95). These examples clearly shed light on the potential of small molecule inhibitors as probes to study ribosome assembly and to uncover the role of new assembly factors. Therefore, even though chemical approaches in combination with cryo-EM hold tremendous promise and offer unique advantages for the study of the ribosome assembly process, current progress is hampered for the limited number of available probes. Nevertheless, the moment is ripe for a collaborative effort to identify specific chemical inhibitors of ribosome assembly that will be of great use as probes (92).

Instead, genetic approaches have been extensively used to investigate the role of assembly factors in ribosome biogenesis. The main approach has consisted in creating single

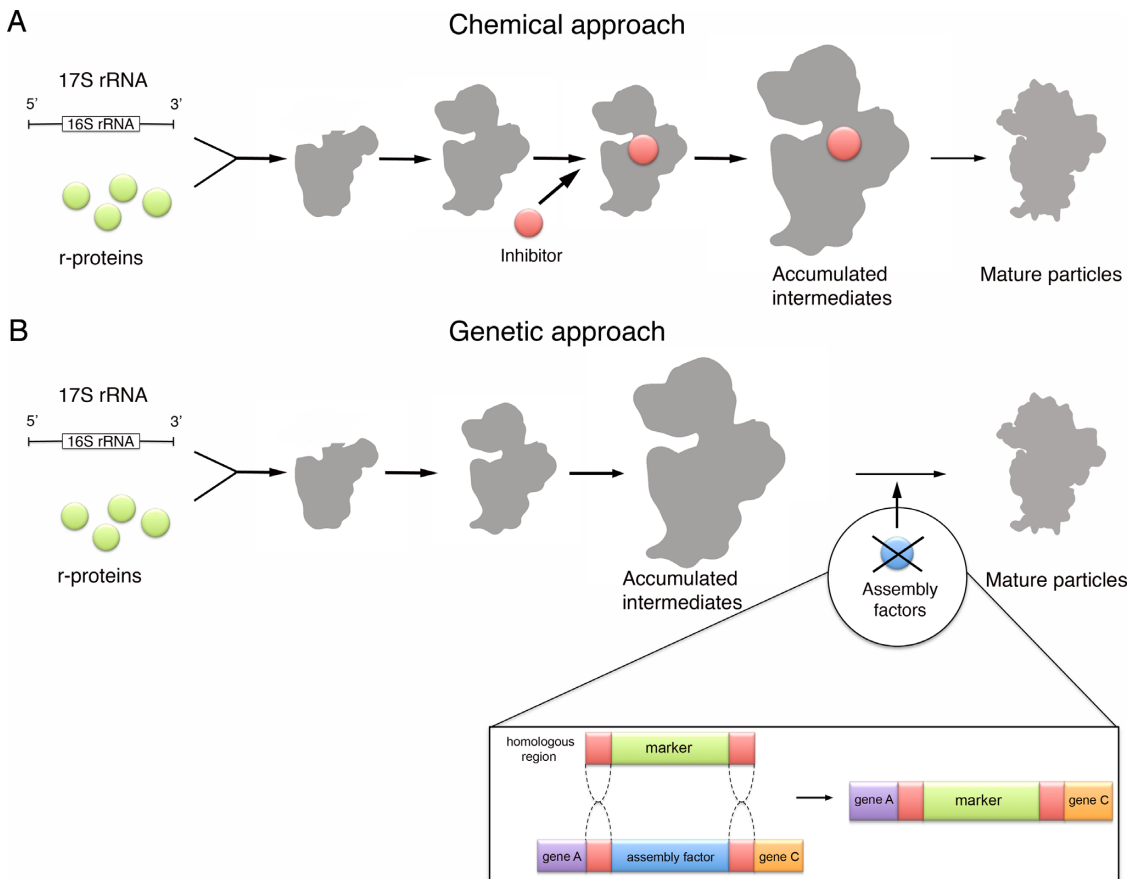


**Figure 4.** Chemical and genetic approaches to capture *in vivo* assembled ribosomal subunit intermediates. (A) The diagram represents the assembly line of the 30S subunit. Chemical approaches use small-molecule inhibitors to block a specific step in the ribosome assembly process, which leads to the accumulation of immature subunits. These particles can be purified and characterized using biochemical or structural methods including cryo-EM. (B) In genetic approaches single-gene deletion strains are created by homologous recombination where the open-reading frame region of the gene for an assembly factor is replaced with a marker cassette. Absence of a particular assembly factor causes a slowdown of the specific assembly steps assisted by this factor, which eventually leads to accumulation of assembly intermediates that are possible to purify for subsequent analysis.

(or double) deletion strains for one of the assembly factors to disable or slow down the ribosome biogenesis process. These strains accumulate immature subunits in sufficient amounts to be isolated and characterized (Figure 4B).

The foundation of this experimental approach is that the ribosomal particles that accumulate upon single deletion of one of these protein factors are informative on the maturation reaction catalyzed by this enzyme. An important premise for this statement is that the ribosomal particles that accumulate constitute the actual substrate for the factor (45–51). However, it is not trivial to confirm this assumption because genetic perturbations cause a steady-state in which, the actual particles that accumulate may have evolved and do not necessarily constitute the actual substrate for the assembly factor. Instead, they may represent particles that have transitioned into a local energy minimum that are thermodynamically stable and off pathway. Ideally, these particles should also be able to mature into functional subunits to rule out that they are not simply dead-end assembly products (Figure 5). It is only recently that a couple of studies (see section 6 below) (96,97) have asked which of these potential scenarios concur in single deletion strains used to capture assembly intermediates.

Despite these caveats, biochemical and structural studies of particles accumulating in single gene deletion strains of assembly factors have provided a great deal of information regarding the function of a group of assembly factors, mainly those involved at the late stages of maturation (45–51). In the next section, we summarize these studies and the significance of their findings.

#### WHAT HAVE WE LEARNED FROM STRUCTURAL STUDIES OF RIBOSOME ASSEMBLY INTERMEDIATES PURIFIED FROM DELETION STRAINS?

Several studies have been published in the last few years where single deletion (or depletion) strains of assembly factors were used to trigger accumulation of assembly intermediates for purification and analysis by cryo-EM. Structural characterization of several late 30S assembly intermediates that accumulate in *Escherichia coli* cells lacking either YjeQ (RsgA) (45), RimM (46,49), KsgA (48) or both YjeQ and RbfA (50) assembly factors revealed that the immature 30S particles that accumulate in these null strains are at the late stages of the maturation process (Figure 1A). Most of the structural motifs of these ribosomal subunits resemble

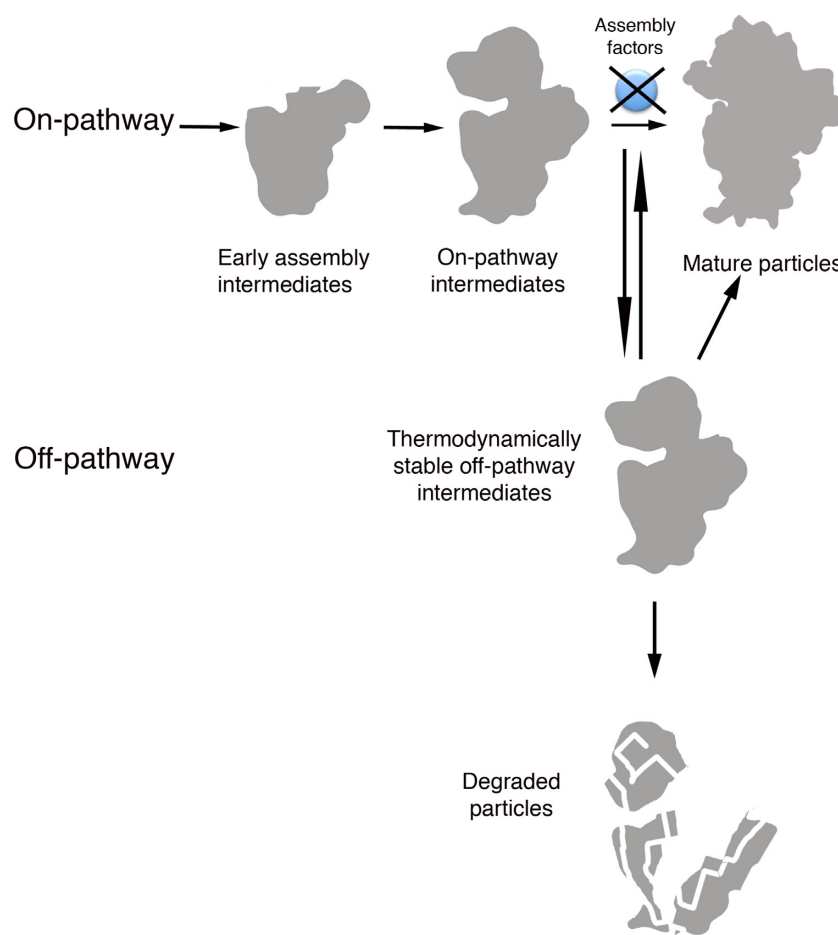


**Figure 5.** Diagram describing the nature of the immature ribosomal particles accumulating in bacterial cells depleted from assembly factors. In the presence of assembly factors, ribosomal assembly progresses normally to produce mature 30S subunits. In the absence of one or multiple assembly factors, it is possible that the assembly intermediate, which represents the actual substrate for the factor remains as such and accumulates (on-pathway intermediate). It is also plausible that the true on-pathway intermediate may be thermodynamically unstable and end up evolving into a more energetically favorable state. This particle then progresses into the immature particles that are observed accumulating in the null strains and eventually into the mature 30S subunits. A fraction of the particles could also be targeted for degradation.

those of the mature 30S subunit, however they all present a severe distortion at the decoding center that renders these ribosomal particles unable to associate with the 50S subunit and engage in translation. These observations, along with cryo-EM structures of either YjeQ, RbfA and Era (another 30S assembly factor) in complex with mature 30S subunits (Figure 1B) (52–55) postulated that these assembly factors bind immature 30S particles at or near the decoding center to assist in the folding of this functional core.

These studies highlight significant differences regarding the late stages of maturation of the prokaryotic small ribosomal subunit with respect to that in eukaryotes. During the late stages of 40S maturation in yeast there are seven stably bound assembly factors: Tsr1, Rio2 and Dim1 bind to the subunit interface, Pno1 and Nob1 to the platform and Enp1 and Ltv1 to the mRNA opening channel. Together, these factors provide a multi-pronged approach to preventing premature translation initiation (98,99). This is necessary because pre-40S particles can bind mRNAs, translation initiation factors and 60S subunits that are present in the cytoplasm at high concentrations. Therefore, these seven

assembly factors cooperate to inhibit each step in the translation initiation pathway.

In bacteria, assembling 30S subunits at the late stages of maturation are also exposed to high concentrations of tRNAs, mRNAs, translation factors and large ribosomal subunits that are present in the cytoplasm. When YjeQ (52,53) and RbfA (55) are bound, they are positioned to block binding of the translation initiation factors IF1 and IF3 (Figure 1B). Similarly, Era binds the anti-Shine Dalgarno sequence at the 3' end of 16S rRNA (54), thus likely preventing mRNA recruitment (Figure 1B). However, in the 30S subunit ligand blocking is also achieved by the structure of the rRNA itself. The cryo-EM structures of the immature 30S<sub>ΔrimM</sub> and 30S<sub>ΔyjeQ</sub> subunits (45,46,49) revealed that the upper domain of helix 44 is dislodged (Figure 1A). Thus, inter-subunit bridges cannot be formed, and the decoding site helix sterically blocks joining with the 50S subunit. Furthermore, the rearrangements of helix 44 distort the decoding site, which is then unable to provide the minor groove interactions critical for productive recognition of aminoacylated tRNA and translation initiation. It is also unclear

whether YjeQ, RbfA, RimM and Era test the functionality of nascent ribosomal subunits by mimicking elements of the translational cycle, as it is the case for some of the eukaryotic assembly factors assisting the maturation of the small ribosomal subunit (98). Therefore, based on what cryo-EM has revealed, several significant differences seem to exist in the way prokaryotic and eukaryotic cells prevent ribosomal subunits from being engaged in translation before their maturation has been completed.

Similar work has also been done with assembly factors involved in the biogenesis of the 50S subunit, including RbgA (47,51), YphC or YsxC (96). These factors are all essential GTPases (100–103). Using *Bacillus subtilis* strains in which one of these three proteins was under the control of an inducible promoter, it was possible to purify incomplete 50S particles that accumulated in the cells under depletion conditions for these factors. Characterization of the immature particles by cryo-EM (Figure 6A) and other techniques, including quantitative mass spectrometry (qMS), revealed that these factors primarily play a role mainly at the late stages of maturation of the 50S subunit. Their role is related to the maturation of the central protuberance and peptidyl transferase center of the 50S subunit (47,51,96).

Overall, analysis of these assembly intermediates revealed that the functional cores of the 30S and 50S ribosomal subunit are the last structural motif to adopt a mature conformation.

Most of these assembly factors acting at these late stages of the process bind to the maturing functional site of the subunits to likely assist their folding. Their coordinated actions also prevent immature particles from prematurely engaging in protein synthesis. The mechanistic insights on how each assembly factor assists in this process and their precise functions remain largely unknown.

Even though most of these structures were obtained before the direct detectors were available and the resolution of these structures is moderate ( $>10$  Å) (Figure 1), these studies clearly illustrate the potential of cryo-EM to visualize in three dimensions the ribosome assembly process.

## LIMITATIONS OF USING RIBOSOME ASSEMBLY INTERMEDIATES ACCUMULATING IN DELETION STRAINS FOR CRYO-EM STUDIES

An important question underlying the use of assembly intermediates accumulating in single deletion (or depletion) strains as samples for cryo-EM structural studies on ribosome assembly is whether these particles can progress to a mature subunit that can associate and form functional 70S ribosomes. In addition, it is also essential to understand the nature of these particles and whether they constitute on-pathway assembly intermediates and true substrate for the assembly factors (Figure 5).

The first study addressing the question of competency for maturation of these immature particles chose to analyze an incomplete 50S particle (45S<sub>RbgA</sub>) (51) purified from a *B. subtilis* strain in which the essential assembly factor RbgA had been depleted (100). Pulse-labeling experiments followed by quantitative mass spectrometry (qMS) demonstrated that the 45S<sub>RbgA</sub> particles that accumulate in the cells under RbgA depletion conditions are competent for

maturity and progress into functional 70S particles. This initial finding provided reassurance that at least some of the particles that accumulate in these depletion strains do not represent a dead-end product of the reaction and thus, they are likely informative about the function of assembly factors (Figure 5).

More recently, a second study (97) performed pulse-chase experiments to test whether the 30S<sub>ΔyjeQ</sub> and 30S<sub>ΔrimM</sub> particles, accumulating in single deletion strains of the YjeQ and RimM assembly factors progress to mature 30S subunits. In these experiments, a discrete population of 17S rRNA that accumulated in the  $\Delta yjeQ$ ,  $\Delta rimM$  and wild type strains was labeled by adding <sup>3</sup>H (tritium)-uracil to the growing culture and the 17S/16S rRNA ratio was used as a proxy to estimate the proportion of immature 30S subunits that progressed to mature 30S subunits. The obtained results were consistent with the progression of at least a substantial proportion (~50%) of the 30S<sub>ΔyjeQ</sub> and 30S<sub>ΔrimM</sub> particles into mature 30S subunits (Figure 5).

Surprisingly, the same study (97) found that affinity binding of assembly factors YjeQ, Era, RbfA and RimM to the 30S<sub>ΔyjeQ</sub> and 30S<sub>ΔrimM</sub> immature particles is weak and that binding would not occur at physiological concentrations. In alignment with these results, mass spectrometry analysis revealed that *in vivo* the occupancy level of these factors in these immature 30S particles is below 10% and that the concentration of factors does not increase when immature particles accumulate in cells. These results suggest that in the absence of these factors, the immature particles evolve into a thermodynamically stable intermediate that exhibits low affinity for the assembly factors (Figure 5). It also implies that the true substrates of YjeQ, RbfA, RimM and Era are immature particles that precede the ribosomal particles accumulating in the knockout strains.

This conclusion aligns well with a presumed role of these factors in chaperoning the folding of rRNA. It seems likely that these assembly factors may play a role in stabilizing specific rRNA motifs at or near the decoding center in certain conformations (52–55,104). In the absence of any of these factors, the conformation of the rRNA motifs that these factors should bind may transition into a local energy minimum that is thermodynamically more stable. The proposed model from this study (97) is that in the single deletion strains the on-pathway intermediate that constitutes the real substrate for each factor progresses to a downstream assembly intermediate that exhibits low affinity to the factors. Indeed, recent studies (45,46,49,50) found that the 30S<sub>ΔyjeQ</sub> and 30S<sub>ΔrimM</sub> particles accumulating in the  $\Delta rimM$  and  $\Delta yjeQ$  null strains are structurally similar. Therefore, it seems that in the knockout strains the different on-pathway intermediates that are recognized by the specific assembly factors may be progressing into a structurally similar local energy minimum intermediate (Figure 5).

A similar study (96) investigated the nature of assembly intermediates in the 50S subunit in *B. subtilis* strains depleted from RbgA, YphC and YsxC. In this study, it was found that these assembly factors bind specifically to the immature particles that the depletion strains accumulate. This result is different from what it was found for the 30S subunit assembly intermediates that accumulate in the absence of YjeQ and RimM (97). These results suggest that the 50S

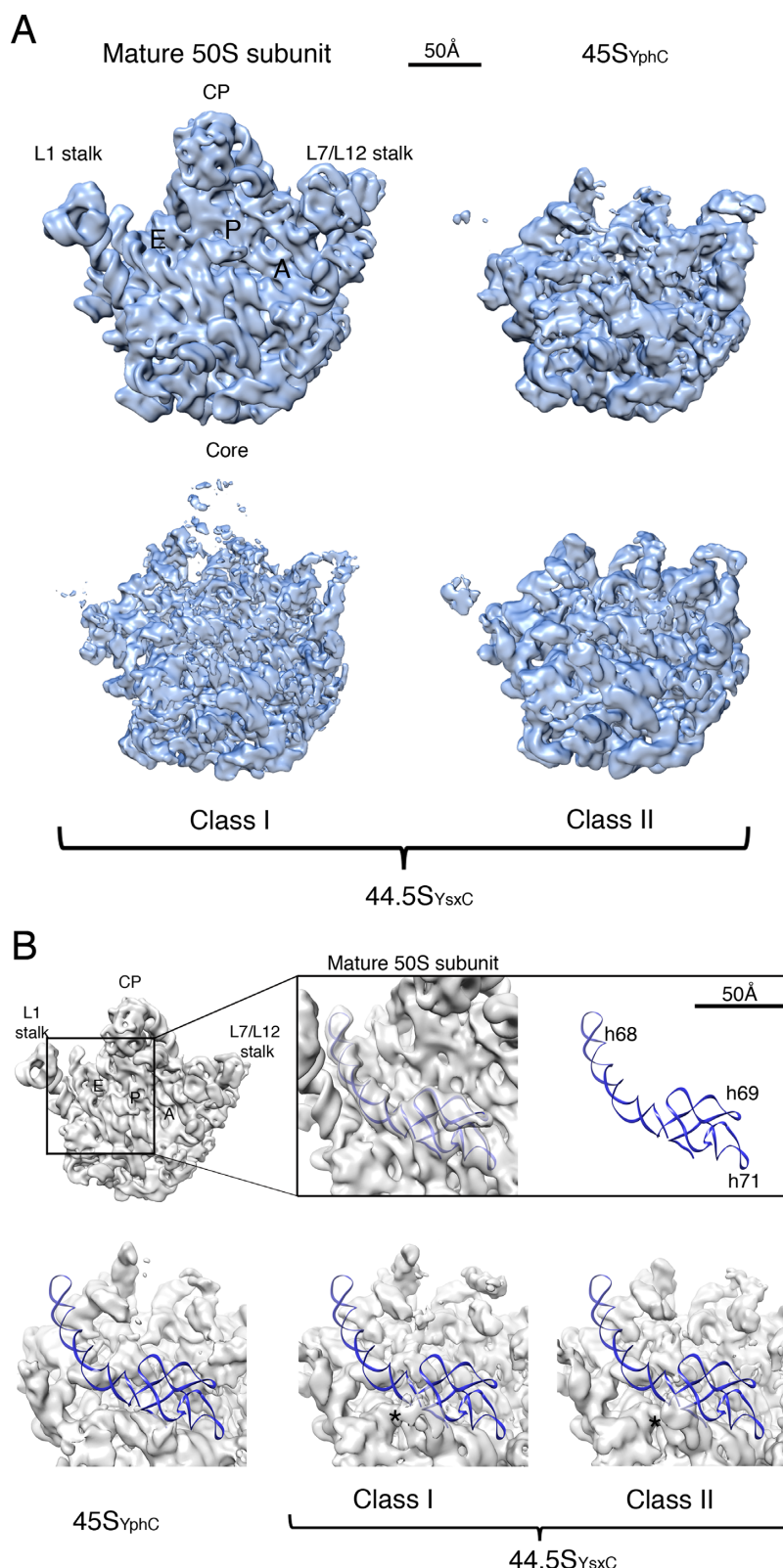


**Figure 6.** Cryo-EM structures of ribosome assembly intermediates obtained using direct electron detector cameras. **(A)** Gallery of cryo-EM structures from assembly intermediates of the 50S subunit from *B. subtilis*. These intermediates accumulate in the cells of *B. subtilis* strains depleted for assembly factors YhpC ( $45S_{YphC}$ ) and YsxC ( $44.5S_{YsxC}$ ). **(B)** The cryo-EM structures obtained with a direct detector are at sufficient resolution to allow identification of individual rRNA helices still remaining in an immature state. This panel shows rRNA helices in the P and E site of the 50S subunit that are not adopting the mature conformation. A corresponding density for these helices is not observed in the density map. The atomic model of the *B. subtilis* 50S subunit (PDB ID: 3j9W) was docked onto the cryo-EM map to indicate the conformation of these rRNA helices in the mature 50S subunit. This figure is a modified version of that in the publication from Ni *et al.* (96).

immature particles constitute either the actual on-pathway substrates or their conformations have not diverged significantly and they are still recognized by the factors (Figure 5). Therefore, the structural differences existing in these immature particles compared to the mature 50S subunit are likely more informative of the function of the assembly factors than those inferred from the 30S assembly intermediates. These two studies (96,97) also indicate interesting differences in the thermodynamic stability of the assembly intermediates of the 30S and 50S subunits.

The fact that assembly factors acting at late stages seem to be playing a role in the stabilization of transient RNA conformations introduces an interesting functional analogy between assembly factors and *bona fide* r-proteins. Should further research provide mechanistic details of the role of the assembly factors as an RNA chaperone, it may suggest that the function for the assembly factors is not substantially different than the function played by r-proteins. An intriguing difference between the two groups of proteins is that *bona fide* r-proteins remain bound to the ribosomal particle, but assembly factors fall off or are removed once their chaperone function has been completed. The fact that their binding site overlaps with important intersubunit bridges that are essential for the association with the 50S subunit (52–55,104) makes necessary their release and it may have driven this functional divergence.

Overall, *in vivo* assembled immature particles accumulated through genetic approaches present several limitations when used for cryo-EM studies to infer about the function of assembly factors. However, particles characterized up to date have still provided a great deal of functional insights about assembly factors and the late stages of assembly.

## OVERCOMING EXISTING LIMITATIONS FOR THE STUDY OF THE RIBOSOME ASSEMBLY PROCESS IN BACTERIA

All assembly intermediates that have been structurally characterized by cryo-EM so far have been purified from single deletion strains or depleted strains lacking individual assembly factors. In addition, most of these structures were obtained from electron micrographs captured either on film or in a CCD and thus, they were only obtained to moderate resolution. Consequently, our current understanding of the function of assembly factors and how these functions are performed in three dimensions is most likely vague at best.

Recent developments in hardware and software for cryo-EM has made possible to obtain the first structures of assembly intermediates in bacteria at a level of detail approaching atomic resolution. An example of the use of these new advancements is a recent publication (96) presenting the structure at ~5 Å resolution of two 50S immature particles obtained upon depletion of YphC and YsxC, two essential assembly factors (Figure 6A). Different from previous moderate-resolution (~10–15 Å) cryo-EM studies (45–47,49–51), the structures obtained from direct detectors allow visualization of individual rRNA helices in the intermediate particles that are still in an immature conformation (Figure 6B). Consequently, these structures are generating testable models regarding the function of protein factors in assembly.

With the technology to obtain atomic resolution structures using cryo-EM of immature ribosomal particles now available, developing methods that have the capability to introduce immediate perturbations in the assembly process and allow rapid capture of these intermediates are much needed to move the field forward. Certainly, chemical approaches and the use of small inhibitor molecules against assembly factors (Figure 4A) hold great promise and are uniquely suited to contribute to our structurally understanding of the sequence of events that leads to assembly of the mature subunits with high temporal precision. The ability of small molecules to target specific functions and to produce perturbations with basically no-lag phase allows for a much simpler interpretation of the structures and the information they convey regarding the function of the targeted factors. Similarly small molecule inhibitors of rRNA-ribosomal protein interactions or rRNA folding events also have great potential for isolation of other structurally valuable intermediates (88). Unfortunately, they do not represent at this moment a realistic option due to the scarcity of effective small molecules available to inhibit specific steps of the ribosome assembly process in bacteria (88).

On the other side, the intrinsic thermodynamic instability of the assembly intermediates that accumulate in cells using current genetic approaches (96,97) requires modifying and extending these methods to be able to achieve purification of the on-pathway assembly intermediates that constitute the true substrate for particular assembly factors. Having these purification methods in place will allow obtaining snapshots of the entire spectrum of states existing in the cell during the ribosome biogenesis process by cryo-EM. However, to what extent the protocols for extraction, purification, and cryo-EM specimen preparation will allow us to obtain an unbiased description of these intermediates states is also an open question that needs to be addressed with considerable urgency.

Recent structural work using direct electron detectors for the structural analysis of ribosome assembly intermediates in yeast (105) is providing examples for potential approaches that could be applied in bacteria and they would likely capture the on-pathway assembly intermediates representing the true substrate of particular assembly factors. In this publication nucleoplasmic pre-60S ribosomal particles were purified by tandem affinity purification after introducing a TAP tag (Figure 7A) in the assembly factor Nog2, which associates with nucleoplasmic pre-60S ribosomal particles. The structure of the purified Nog2 particles was solved to ~3 Å resolution using cryo-EM and showed over 20 different assembly factors bound mainly to an arc region extending from the central protuberance to the polypeptide tunnel exit and the domain called internal transcribed space 2. Guided by chemical cross-linking of proteins coupled with mass spectrometry, it was possible to build the atomic model for 19 of the assembly factors bound to the assembly intermediate.

Considering that in this work the TAP-Nog2 factor was expressed at close to physiological concentrations and that in the tandem affinity purification the tagged factor recovered under native conditions along with associated partners, it is quite likely that this remarkable structure has a close resemblance to the on-pathway assembly intermediate that

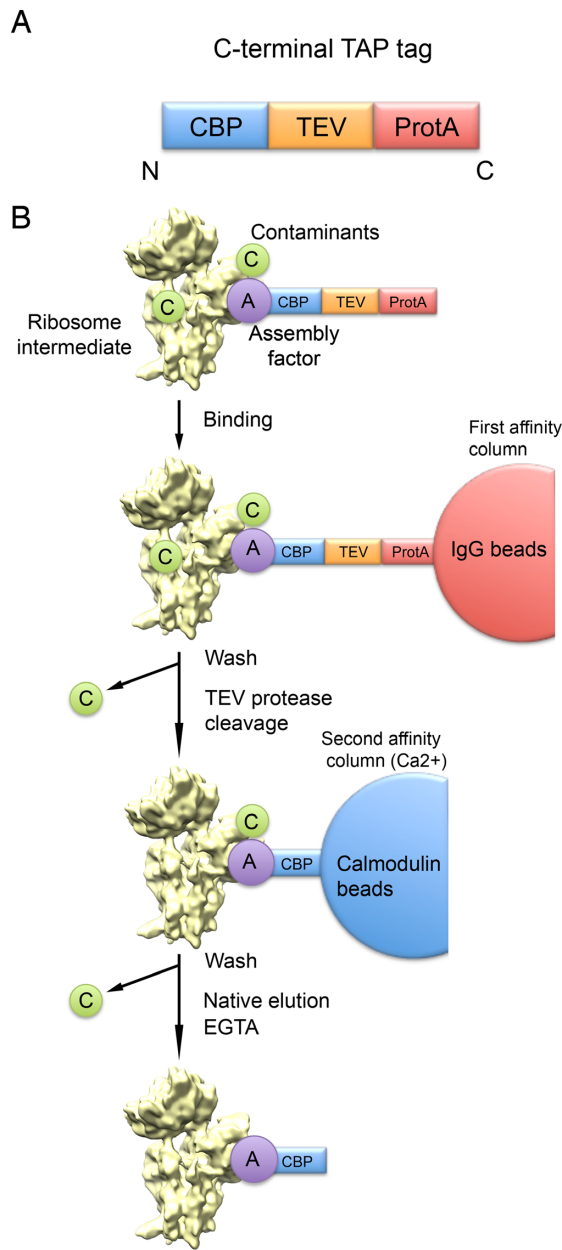


**Figure 7.** Tandem affinity purification (TAP) as a method for purification of ribosome assembly intermediates. (A) Schematic of the C-terminal tag used for TAP. The tag consists of protein A (ProtA) and a calmodulin binding peptide (CBP) separated by a Tobacco Etch Virus (TEV) protease cleavage site. (B) Overview of the TAP strategy for purification of ribosome assembly intermediates. This method requires the fusion of the TAP tag to the C-terminal end of the target protein (assembly factor) and introduction of this construct into the host cell. Upon induction the tagged assembly factor will interact with the assembly intermediate (true substrate) in the cells. Cell extracts are prepared and passed through two affinity purification steps. In the first step, ProtA binds tightly to an IgG matrix carrying along the assembly factor in complex with the immature subunit. However, contaminants are washed away. Elution from this column is attained by cleaving the construct with TEV protease. The eluted complex is then loaded in a second column containing calmodulin beads, which have high affinity for the CBP module on the TAP tag (CBP). Additional washes allow for further removal of contaminating proteins. Final elution is achieved under mild conditions with EGTA. All buffer conditions used during this procedure are mild. Therefore, the obtained purified assembly factor in complex with the immature ribosomal particle is eluted under native conditions.

constitutes the true substrate of these assembly factors and that bacterial studies have endeavored to capture, so far with much more limited success.

Tandem affinity purification (Figure 7) was initially developed in yeast, but has been subsequently employed successfully in the analysis of protein–protein interactions and protein complexes in other organisms including mammals, plants, *Drosophila* and more importantly for the work discussed here, also in bacteria. At this point, only a limited number of examples exist in the usage of tandem affinity purification for characterization of protein complexes in bacteria. A few instances include, Gully *et al.* that first used this approach to isolate native protein complexes (106) and Shereda *et al.* (107) that employed this method to purify the RecQ complex and identified three new heterologous proteins that associate with this complex. The most relevant example for the prospects of using tandem affinity purification for the study of ribosome biogenesis in bacteria was work from the same laboratory (108) that discovered the formation of a specific ribonucleoprotein complex between SrmB, a DEAD-box protein, and ribosomal proteins uL4, uL24 and the 5' region of the 23S rRNA. All of these examples provide exciting prospects for the use of this purification method for capturing on-pathway assembly intermediates that constitute the true substrate of particular assembly factors.

The incorporation of tags in the rRNA has been a recent successful approach for the purification of *in vivo* assembled immature ribosomal particles in bacteria. Gupta *et al.* (109) devised a strategy for purification of pre-16S rRNA-containing assembly intermediates of the 30S subunit. In this approach, an MS2 bacteriophage RNA stem-loop was placed at different positions in the 5' or 3' precursor sequences of the 17S rRNA and used for affinity purification using beads pre-bound with MS2 fusion protein. The different location of the MS2 tag led to the purification of three intermediates, each one of them containing different length of the 5' or 3' precursor sequences.

Exploring the conformation of the precursor 16S rRNA in these intermediates using chemical probing revealed, similar to the cryo-EM studies from single deletion strains of assembly factors (45,46,48,49) that these particles are at the late stages of maturation and all lack mature functional sites. Similarly, they were also depleted of some of late binding r-proteins that enter late in the assembly; in particular uS2, uS3 and bS21 were severely underrepresented in all of these intermediates. An important conclusion of this work is that the 17S rRNA acts as a major scaffold for 30S subunit biogenesis, which occurs following multiple assembly pathways. More importantly, this MS2-tag based purification method also offers a number of *in vivo* snapshots of assembling 30S subunits, however they have yet to be characterized by cryo-EM. Only then, it will be possible to determine their potential to contribute to our understanding of the late stages of maturation of the 30S subunit and the structural aspects related to the processing of the precursor sequences of the 17S rRNA.

Finally, a recent review paper (88) has also proposed the idea of using small molecule inhibitors as affinity purification tags for low abundance ribosomal intermediates. Once effective small molecule inhibitors of the ribosome matura-

tion process become available, this approach will certainly represent an exciting alternative to the tandem affinity purification method described above for purification of on-pathway immature particles indicated above. The small size of molecular inhibitors makes them less likely to introduce structural artifacts upon perturbations in assembly.

## FUTURE PERSPECTIVES AND CONCLUSION

Since the development of the vitrification process by Dubochet and colleagues (16) in 1984, cryo-EM has been an essential contributor to the structure and function of the ribosome. The recent developments in hardware and software and new emerging methods to capture on-pathway ribosome assembly intermediates in complex with assembly factors are currently positioning cryo-EM to make tremendous contributions to the understanding of the ribosome assembly process in bacteria. Undoubtedly, the rich structural information contained in the structures that cryo-EM will produce in the upcoming years using these new developments will provide an extremely valuable framework for the dissection of the molecular roles and function of assembly factors involved in the maturation of the two ribosomal subunits. Furthermore, these structures will provide an effective platform to develop new antibiotics against this fundamental cellular process and pave the way to use these assembly factors as antimicrobial targets. Finally, the fact that some of the bacterial GTPases functioning as assembly factors have eukaryotic counterparts (69) ensures that some of the new insights brought by cryo-EM about the assembly process in bacteria will also provide new therapeutic opportunities for cancer.

## ACKNOWLEDGEMENTS

We are grateful to our collaborators in the field of ribosome biogenesis including Drs. James Williamson, Eric Brown and Joseph Davis for invigorating discussion over the years. We also thank Dr. Brett Thurlow for insightful comments on this manuscript. We are also in debt to Dr. John Rubinstein for generously giving us access to the electron microscopy facility at the Hospital for Sick Children in Toronto.

## FUNDING

National Science and Engineering Research Council of Canada [RGPIN288327-07]; Canadian Institutes of Health Research (CIHR) [MOP-82930 to J.O.]; National Institutes of Health [1R01GM110248 to R.A.B.]. Funding for open access charge: CIHR.

*Conflict of interest statement.* None declared.

## REFERENCES

- Schluelzen,F., Tocilj,A., Zarivach,R., Harms,J., Gluehmann,M., Janell,D., Bashan,A., Bartels,H., Agmon,I., Franceschi,F. *et al.* (2000) Structure of functionally activated small ribosomal subunit at 3.3 angstroms resolution. *Cell*, **102**, 615–623.
- Wimberly,B.T., Brodersen,D.E., Clemons,W.M. Jr, Morgan-Warren,R.J., Carter,A.P., Vonrhein,C., Hartsch,T. and Ramakrishnan,V. (2000) Structure of the 30S ribosomal subunit. *Nature*, **407**, 327–339.
- Ban,N., Nissen,P., Hansen,J., Moore,P.B. and Steitz,T.A. (2000) The complete atomic structure of the large ribosomal subunit at 2.4 Å resolution. *Science*, **289**, 905–920.
- Tischendorf,G.W., Zeichhardt,H. and Stoffler,G. (1974) Location of proteins S5, S13 and S14 on the surface of the 30S ribosomal subunit from *Escherichia coli* as determined by immune electron microscopy. *Mol. Gen. Genet.*, **134**, 209–223.
- Tischendorf,G.W., Zeichhardt,H. and Stoffler,G. (1974) Determination of the location of proteins L14, L17, L18, L19, L22, L23 on the surface of the 50S ribosomal subunit of *Escherichia coli* by immune electron microscopy. *Mol. Gen. Genet.*, **134**, 187–208.
- Branlant,C., Krol,A., Sriwidada,J. and Brimacombe,R. (1976) RNA sequences associated with proteins L1, L9, and L5, L18, L25, in ribonucleoprotein fragments isolated from the 50-S subunit of *Escherichia coli* ribosomes. *Eur. J. Biochem.*, **70**, 483–492.
- Brimacombe,R., Nierhaus,K.H., Garrett,R.A. and Wittmann,H.G. (1976) The ribosome of *Escherichia coli*. *Prog. Nucleic Acid Res. Mol. Biol.*, **18**, 323–325.
- Rinke,J., Yuki,A. and Brimacombe,R. (1976) Studies on the environment of protein S7 within the 30-S subunit *Escherichia coli* ribosomes. *Eur. J. Biochem.*, **64**, 77–89.
- Capel,M.S., Engelman,D.M., Freeborn,B.R., Kjeldgaard,M., Langer,J.A., Ramakrishnan,V., Schindler,D.G., Schneider,D.K., Schoenborn,B.P., Sillers,I.Y. *et al.* (1987) A complete mapping of the proteins in the small ribosomal subunit of *Escherichia coli*. *Science*, **238**, 1403–1406.
- Fox,G.E. and Woese,C.R. (1975) The architecture of 5S rRNA and its relation to function. *J. Mol. Evol.*, **6**, 61–76.
- Noller,H.F. and Woese,C.R. (1981) Secondary structure of 16S ribosomal RNA. *Science*, **212**, 403–411.
- Woese,C.R., Gutell,R., Gupta,R. and Noller,H.F. (1983) Detailed analysis of the higher-order structure of 16S-like ribosomal ribonucleic acids. *Microbiol. Rev.*, **47**, 621–669.
- Woese,C.R., Winkler,S. and Gutell,R.R. (1990) Architecture of ribosomal RNA: constraints on the sequence of “tetra-loops”. *Proc. Natl. Acad. Sci. U.S.A.*, **87**, 8467–8471.
- Gutell,R.R. and Woese,C.R. (1990) Higher order structural elements in ribosomal RNAs: pseudo-knots and the use of noncanonical pairs. *Proc. Natl. Acad. Sci. U.S.A.*, **87**, 663–667.
- Gutell,R.R., Weiser,B., Woese,C.R. and Noller,H.F. (1985) Comparative anatomy of 16S-like ribosomal RNA. *Prog. Nucleic Acid Res. Mol. Biol.*, **32**, 155–216.
- Dubochet,J., Adrian,M., Chang,J.J., Homo,J.C., Lepault,J., McDowall,A.W. and Schultz,P. (1988) Cryo-electron microscopy of vitrified specimens. *Q. Rev. Biophys.*, **21**, 129–228.
- Frank,J. (1995) Approaches to large-scale structures. *Curr. Opin. Struct. Biol.*, **5**, 194–201.
- Williamson,J.R. (2009) The ribosome at atomic resolution. *Cell*, **139**, 1041–1043.
- Munro,J.B., Sanbonmatsu,K.Y., Spahn,C.M. and Blanchard,S.C. (2009) Navigating the ribosome’s metastable energy landscape. *Trends Biochem. Sci.*, **34**, 390–400.
- Frank,J. and Gonzalez,R.L. Jr (2010) Structure and dynamics of a processive Brownian motor: the translating ribosome. *Annu. Rev. Biochem.*, **79**, 381–412.
- Mitra,K. and Frank,J. (2006) Ribosome dynamics: insights from atomic structure modeling into cryo-electron microscopy maps. *Annu. Rev. Biophys. Biomol. Struct.*, **35**, 299–317.
- Sigworth,F.J. (1998) A maximum-likelihood approach to single-particle image refinement. *J. Struct. Biol.*, **122**, 328–339.
- Scheres,S.H., Nunez-Ramirez,R., Gomez-Llorente,Y., San Martin,C., Eggermont,P.P. and Carazo,J.M. (2007) Modeling experimental image formation for likelihood-based classification of electron microscopy data. *Structure*, **15**, 1167–1177.
- Scheres,S.H., Valle,M. and Carazo,J.M. (2005) Fast maximum-likelihood refinement of electron microscopy images. *Bioinformatics*, **21**(Suppl. 2), ii243–ii244.
- Scheres,S.H., Valle,M., Nunez,R., Sorzano,C.O., Marabini,R., Herman,G.T. and Carazo,J.M. (2005) Maximum-likelihood multi-reference refinement for electron microscopy images. *J. Mol. Biol.*, **348**, 139–149.
- Henderson,R. (2004) Realizing the potential of electron cryo-microscopy. *Q. Rev. Biophys.*, **37**, 3–13.

27. Henderson,R. (2015) Overview and future of single particle electron cryomicroscopy. *Arch. Biochem. Biophys.*, **581**, 19–24.
28. Baker,T.S. and Johnson,J.E. (1996) Low resolution meets high: towards a resolution continuum from cells to atoms. *Curr. Opin. Struct. Biol.*, **6**, 585–594.
29. Grigorieff,N. (2013) Direct detection pays off for electron cryo-microscopy. *eLife*, **2**, e00573.
30. Li,X., Mooney,P., Zheng,S., Booth,C.R., Braunfeld,M.B., Gubbens,S., Agard,D.A. and Cheng,Y. (2013) Electron counting and beam-induced motion correction enable near-atomic-resolution single-particle cryo-EM. *Nat. Methods*, **10**, 584–590.
31. Ruskin,R.S., Yu,Z. and Grigorieff,N. (2013) Quantitative characterization of electron detectors for transmission electron microscopy. *J. Struct. Biol.*, **184**, 385–393.
32. Voorhees,R.M., Fernandez,I.S., Scheres,S.H. and Hegde,R.S. (2014) Structure of the mammalian ribosome-Sec 61 complex to 3.4 Å resolution. *Cell*, **157**, 1632–1643.
33. Wong,W., Bai,X.C., Brown,A., Fernandez,I.S., Hanssen,E., Condron,M., Tan,Y.H., Baum,J. and Scheres,S.H. (2014) Cryo-EM structure of the Plasmodium falciparum 80S ribosome bound to the anti-protozoan drug emetine. *eLife*, **3**, doi:10.7554/eLife.03080.
34. Fischer,N., Neumann,P., Konevega,A.L., Bock,L.V., Ficner,R., Rodnina,M.V. and Stark,H. (2015) Structure of the E. coli ribosome-EF-Tu complex at <3 Å resolution by Cs-corrected cryo-EM. *Nature*, **520**, 567–570.
35. Greber,B.J., Boehringer,D., Leibundgut,M., Bieri,P., Leitner,A., Schmitz,N., Aebersold,R. and Ban,N. (2014) The complete structure of the large subunit of the mammalian mitochondrial ribosome. *Nature*, **515**, 283–286.
36. Khatter,H., Myasnikov,A.G., Natchiar,S.K. and Klaholz,B.P. (2015) Structure of the human 80S ribosome. *Nature*, **520**, 640–645.
37. Traub,P. and Nomura,M. (1968) Structure and function of Escherichia coli ribosomes. I. Partial fractionation of the functionally active ribosomal proteins and reconstitution of artificial subribosomal particles. *J. Mol. Biol.*, **34**, 575–593.
38. Traub,P. and Nomura,M. (1968) Structure and function of E. coli ribosomes. V. Reconstitution of functionally active 30S ribosomal particles from RNA and proteins. *Proc. Natl. Acad. Sci. U.S.A.*, **59**, 777–784.
39. Traub,P. and Nomura,M. (1969) Structure and function of Escherichia coli ribosomes. VI. Mechanism of assembly of 30 s ribosomes studied in vitro. *J. Mol. Biol.*, **40**, 391–413.
40. Traub,P. and Nomura,M. (1969) Studies on the assembly of ribosomes in vitro. *Cold Spring Harb. Symp. Quant. Biol.*, **34**, 63–67.
41. Traub,P., Soll,D. and Nomura,M. (1968) Structure and function of Escherichia coli ribosomes. II. Translational fidelity and efficiency in protein synthesis of a protein-deficient subribosomal particle. *J. Mol. Biol.*, **34**, 595–608.
42. Dietrich,S., Schrandt,I. and Nierhaus,K.H. (1974) Interdependence of E. coli ribosomal proteins at the peptidyltransferase centre. *FEBS Lett.*, **47**, 136–139.
43. Nierhaus,K.H. and Dohme,F. (1974) Total reconstitution of functionally active 50S ribosomal subunits from Escherichia coli. *Proc. Natl. Acad. Sci. U.S.A.*, **71**, 4713–4717.
44. Nierhaus,K.H. and Dohme,F. (1979) Total reconstitution of 50 S subunits from Escherichia coli ribosomes. *Methods Enzymol.*, **59**, 443–449.
45. Jomaa,A., Stewart,G., Martin-Benito,J., Zielke,R., Campbell,T.L., Maddock,J.R., Brown,E.D. and Ortega,J. (2011) Understanding ribosome assembly: the structure of in vivo assembled immature 30S subunits revealed by cryo-electron microscopy. *RNA*, **17**, 697–709.
46. Leong,V., Kent,M., Jomaa,A. and Ortega,J. (2013) Escherichia coli rimM and yjeQ null strains accumulate immature 30S subunits of similar structure and protein complement. *RNA*, **19**, 789–802.
47. Li,N., Chen,Y., Guo,Q., Zhang,Y., Yuan,Y., Ma,C., Deng,H., Lei,J. and Gao,N. (2013) Cryo-EM structures of the late-stage assembly intermediates of the bacterial 50S ribosomal subunit. *Nucleic Acids Res.*, **41**, 7073–7083.
48. Boehringer,D., O'Farrell,H.C., Rife,J.P. and Ban,N. (2012) Structural insights into methyltransferase KsgA function in 30S ribosomal subunit biogenesis. *J. Biol. Chem.*, **287**, 10453–10459.
49. Guo,Q., Goto,S., Chen,Y., Feng,B., Xu,Y., Muto,A., Himeno,H., Deng,H., Lei,J. and Gao,N. (2013) Dissecting the in vivo assembly of the 30S ribosomal subunit reveals the role of RimM and general features of the assembly process. *Nucleic Acids Res.*, **41**, 2609–2620.
50. Yang,Z., Guo,Q., Goto,S., Chen,Y., Li,N., Yan,K., Zhang,Y., Muto,A., Deng,H., Himeno,H. et al. (2014) Structural insights into the assembly of the 30S ribosomal subunit in vivo: functional role of S5 and location of the 17S rRNA precursor sequence. *Protein Cell*, **5**, 394–407.
51. Jomaa,A., Jain,N., Davis,J.H., Williamson,J.R., Britton,R.A. and Ortega,J. (2014) Functional domains of the 50S subunit mature late in the assembly process. *Nucleic Acids Res.*, **42**, 3419–3435.
52. Jomaa,A., Stewart,G., Mears,J.A., Kireeva,I., Brown,E.D. and Ortega,J. (2011) Cryo-electron microscopy structure of the 30S subunit in complex with the YjeQ biogenesis factor. *RNA*, **17**, 2026–2038.
53. Guo,Q., Yuan,Y., Xu,Y., Feng,B., Liu,L., Chen,K., Sun,M., Yang,Z., Lei,J. and Gao,N. (2011) Structural basis for the function of a small GTPase RsgA on the 30S ribosomal subunit maturation revealed by cryoelectron microscopy. *Proc. Natl. Acad. Sci. U.S.A.*, **108**, 13100–13105.
54. Sharma,M.R., Barat,C., Wilson,D.N., Booth,T.M., Kawazoe,M., Hori-Takemoto,C., Shirouzu,M., Yokoyama,S., Fucini,P. and Agrawal,R.K. (2005) Interaction of Era with the 30S ribosomal subunit implications for 30S subunit assembly. *Mol. Cell*, **18**, 319–329.
55. Datta,P.P., Wilson,D.N., Kawazoe,M., Swami,N.K., Kaminishi,T., Sharma,M.R., Booth,T.M., Takemoto,C., Fucini,P., Yokoyama,S. et al. (2007) Structural aspects of RbfA action during small ribosomal subunit assembly. *Mol. Cell*, **28**, 434–445.
56. Ban,N., Beckmann,R., Cate,J.H., Dinman,J.D., Dragon,F., Ellis,S.R., Lafontaine,D.L., Lindahl,L., Liljas,A., Lipton,J.M. et al. (2014) A new system for naming ribosomal proteins. *Curr. Opin. Struct. Biol.*, **24**, 165–169.
57. Srivastava,A.K. and Schlessinger,D. (1990) Mechanism and regulation of bacterial ribosomal RNA processing. *Annu. Rev. Microbiol.*, **44**, 105–129.
58. Hosokawa,K., Fujimura,R.K. and Nomura,M. (1966) Reconstitution of functionally active ribosomes from inactive subparticles and proteins. *Proc. Natl. Acad. Sci. U.S.A.*, **55**, 198–204.
59. Rohl,R. and Nierhaus,K.H. (1982) Assembly map of the large subunit (50S) of Escherichia coli ribosomes. *Proc. Natl. Acad. Sci. U.S.A.*, **79**, 729–733.
60. Herold,M. and Nierhaus,K.H. (1987) Incorporation of six additional proteins to complete the assembly map of the 50 S subunit from Escherichia coli ribosomes. *J. Biol. Chem.*, **262**, 8826–8833.
61. Adilakshmi,T., Bellur,D.L. and Woodson,S.A. (2008) Concurrent nucleation of 16S folding and induced fit in 30S ribosome assembly. *Nature*, **455**, 1268–1272.
62. Talkington,M.W., Siuzdak,G. and Williamson,J.R. (2005) An assembly landscape for the 30S ribosomal subunit. *Nature*, **438**, 628–632.
63. Woodson,S.A. (2008) RNA folding and ribosome assembly. *Curr. Opin. Chem. Biol.*, **12**, 667–673.
64. Woodson,S.A. (2011) RNA folding pathways and the self-assembly of ribosomes. *Acc. Chem. Res.*, **44**, 1312–1319.
65. Kim,H., Abeyasingheunawardena,S.C., Chen,K., Mayerle,M., Ragunathan,K., Luthey-Schulten,Z., Ha,T. and Woodson,S.A. (2014) Protein-guided RNA dynamics during early ribosome assembly. *Nature*, **506**, 334–338.
66. Connolly,K. and Culver,G. (2009) Deconstructing ribosome construction. *Trends Biochem. Sci.*, **34**, 256–263.
67. Shahani,Z., Sykes,M.T. and Williamson,J.R. (2011) Assembly of bacterial ribosomes. *Annu. Rev. Biochem.*, **80**, 501–526.
68. Wilson,D.N. and Nierhaus,K.H. (2007) The weird and wonderful world of bacterial ribosome regulation. *Crit. Rev. Biochem. Mol. Biol.*, **42**, 187–219.
69. Britton,R.A. (2009) Role of GTPases in bacterial ribosome assembly. *Annu. Rev. Microbiol.*, **63**, 155–176.
70. Brown,E.D. (2005) Conserved P-loop GTPases of unknown function in bacteria: an emerging and vital ensemble in bacterial physiology. *Biochem. Cell Biol.*, **83**, 738–746.
71. Orlova,E.V. (2000) Structural analysis of non-crystalline macromolecules: the ribosome. *Acta Crystallogr. D Biol. Crystallogr.*, **56**, 1253–1258.

72. Orlova,E.V. and Saibil,H.R. (2011) Structural analysis of macromolecular assemblies by electron microscopy. *Chem. Rev.*, **111**, 7710–7748.
73. Scheres,S.H., Nunez-Ramirez,R., Sorzano,C.O., Carazo,J.M. and Marabini,R. (2008) Image processing for electron microscopy single-particle analysis using XMIPP. *Nat. Protoc.*, **3**, 977–990.
74. Scheres,S.H. (2012) RELION: implementation of a Bayesian approach to cryo-EM structure determination. *J. Struct. Biol.*, **180**, 519–530.
75. Lyumkis,D., Brilot,A.F., Theobald,D.L. and Grigorieff,N. (2013) Likelihood-based classification of cryo-EM images using FREALIGN. *J. Struct. Biol.*, **183**, 377–388.
76. Bammes,B.E., Rochat,R.H., Jakana,J. and Chiu,W. (2011) Practical performance evaluation of a 10k x 10k CCD for electron cryo-microscopy. *J. Struct. Biol.*, **175**, 384–393.
77. Booth,C.R., Jakana,J. and Chiu,W. (2006) Assessing the capabilities of a 4kx4k CCD camera for electron cryo-microscopy at 300kV. *J. Struct. Biol.*, **156**, 556–563.
78. Bammes,B.E., Rochat,R.H., Jakana,J., Chen,D.H. and Chiu,W. (2012) Direct electron detection yields cryo-EM reconstructions at resolutions beyond 3/4 Nyquist frequency. *J. Struct. Biol.*, **177**, 589–601.
79. Glaeser,R.M. and Hall,R.J. (2011) Reaching the information limit in cryo-EM of biological macromolecules: experimental aspects. *Biophys. J.*, **100**, 2331–2337.
80. Glaeser,R.M., McMullan,G., Faruqi,A.R. and Henderson,R. (2011) Images of paraffin monolayer crystals with perfect contrast: minimization of beam-induced specimen motion. *Ultramicroscopy*, **111**, 90–100.
81. Rubinstein,J.L. and Brubaker,M.A. (2015) Alignment of cryo-EM movies of individual particles by optimization of image translations. *J. Struct. Biol.*, **192**, 188–195.
82. Brilot,A.F., Chen,J.Z., Cheng,A., Pan,J., Harrison,S.C., Potter,C.S., Carragher,B., Henderson,R. and Grigorieff,N. (2012) Beam-induced motion of vitrified specimen on holey carbon film. *J. Struct. Biol.*, **177**, 630–637.
83. Sohmen,D., Chiba,S., Shimokawa-Chiba,N., Innis,C.A., Berninghausen,O., Beckmann,R., Ito,K. and Wilson,D.N. (2015) Structure of the *Bacillus subtilis* 70S ribosome reveals the basis for species-specific stalling. *Nat. Commun.*, **6**, 6941.
84. Amunts,A., Brown,A., Bai,X.C., Llacer,J.L., Hussain,T., Emsley,P., Long,F., Murshudov,G., Scheres,S.H. and Ramakrishnan,V. (2014) Structure of the yeast mitochondrial large ribosomal subunit. *Science*, **343**, 1485–1489.
85. Bai,X.C., Fernandez,I.S., McMullan,G. and Scheres,S.H. (2013) Ribosome structures to near-atomic resolution from thirty thousand cryo-EM particles. *eLife*, **2**, e00461.
86. Mulder,A.M., Yoshioka,C., Beck,A.H., Bunner,A.E., Milligan,R.A., Potter,C.S., Carragher,B. and Williamson,J.R. (2010) Visualizing ribosome biogenesis: parallel assembly pathways for the 30S subunit. *Science*, **330**, 673–677.
87. Lindahl,L. (1975) Intermediates and time kinetics of the in vivo assembly of *Escherichia coli* ribosomes. *J. Mol. Biol.*, **92**, 15–37.
88. Stokes,J.M. and Brown,E.D. (2015) Chemical modulators of ribosome biogenesis as biological probes. *Nat. Chem. Biol.*, **11**, 924–932.
89. Wilson,D.N. (2009) The A-Z of bacterial translation inhibitors. *Crit. Rev. Biochem. Mol. Biol.*, **44**, 393–433.
90. Wilson,D.N. (2014) Ribosome-targeting antibiotics and mechanisms of bacterial resistance. *Nat. Rev. Microbiol.*, **12**, 35–48.
91. Champney,W.S. (2006) The other target for ribosomal antibiotics: inhibition of bacterial ribosomal subunit formation. *Infect. Disord. Drug Targets*, **6**, 377–390.
92. Stokes,J.M., Davis,J.H., Mangat,C.S., Williamson,J.R. and Brown,E.D. (2014) Discovery of a small molecule that inhibits bacterial ribosome biogenesis. *eLife*, **3**, e03574.
93. Loibl,M., Klein,I., Praties,M., Schmidt,C., Kappel,L., Zisser,G., Gungl,A., Krieger,E., Pertschy,B. and Bergler,H. (2014) The drug diazaborine blocks ribosome biogenesis by inhibiting the AAA-ATPase Drg1. *J. Biol. Chem.*, **289**, 3913–3922.
94. Drygin,D., Lin,A., Bliesath,J., Ho,C.B., O'Brien,S.E., Proffitt,C., Omori,M., Haddach,M., Schwaebe,M.K., Siddiqui-Jain,A. et al. (2011) Targeting RNA polymerase I with an oral small molecule CX-5461 inhibits ribosomal RNA synthesis and solid tumor growth. *Cancer Res.*, **71**, 1418–1430.
95. Drygin,D., Siddiqui-Jain,A., O'Brien,S., Schwaebe,M., Lin,A., Bliesath,J., Ho,C.B., Proffitt,C., Trent,K., Whitten,J.P. et al. (2009) Anticancer activity of CX-3543: a direct inhibitor of rRNA biogenesis. *Cancer Res.*, **69**, 7653–7661.
96. Ni,X., Davis,J.H., Jain,N., Razi,A., Benlekbir,S., McArthur,A.G., Rubinstein,J.L., Britton,R.A., Williamson,J.R. and Ortega,J. (2016) YphC and YsxC GTPases assist the maturation of the central protuberance, GTPase associated region and functional core of the 50S ribosomal subunit. *Nucleic Acids Res.*, **44**, 8442–8455.
97. Thurlow,B., Davis,J.H., Leong,V., Moraes,T.F., Williamson,J.R. and Ortega,J. (2016) Binding properties of YjeQ (RsgA), RbfA, RimM and Era to assembly intermediates of the 30S subunit. *Nucleic Acids Res.*, **44**, 9918–9932.
98. Strunk,B.S., Novak,M.N., Young,C.L. and Karbstein,K. (2012) A translation-like cycle is a quality control checkpoint for maturing 40S ribosome subunits. *Cell*, **150**, 111–121.
99. Karbstein,K. (2013) Quality control mechanisms during ribosome maturation. *Trends Cell Biol.*, **23**, 242–250.
100. Uicker,W.C., Schaefer,L. and Britton,R.A. (2006) The essential GTPase RbgA (YlqF) is required for 50S ribosome assembly in *Bacillus subtilis*. *Mol. Microbiol.*, **59**, 528–540.
101. Uicker,W.C., Schaefer,L., Koenigsknecht,M. and Britton,R.A. (2007) The essential GTPase YqeH is required for proper ribosome assembly in *Bacillus subtilis*. *J. Bacteriol.*, **189**, 2926–2929.
102. Matsuo,Y., Morimoto,T., Kuwano,M., Loh,P.C., Oshima,T. and Ogasawara,N. (2006) The GTP-binding protein YlqF participates in the late step of 50 S ribosomal subunit assembly in *Bacillus subtilis*. *J. Biol. Chem.*, **281**, 8110–8117.
103. Schaefer,L., Uicker,W.C., Wicker-Planquart,C., Foucher,A.E., Jault,J.M. and Britton,R.A. (2006) Multiple GTPases participate in the assembly of the large ribosomal subunit in *Bacillus subtilis*. *J. Bacteriol.*, **188**, 8252–8258.
104. Lovgren,J.M., Bylund,G.O., Srivastava,M.K., Lundberg,L.A., Persson,O.P., Wingsle,G. and Wikstrom,P.M. (2004) The PRC-barrel domain of the ribosome maturation protein RimM mediates binding to ribosomal protein S19 in the 30S ribosomal subunits. *RNA*, **10**, 1798–1812.
105. Wu,S., Tutuncuoglu,B., Yan,K., Brown,H., Zhang,Y., Tan,D., Gamalinda,M., Yuan,Y., Li,Z., Jakovljevic,J. et al. (2016) Diverse roles of assembly factors revealed by structures of late nuclear pre-60S ribosomes. *Nature*, **534**, 133–137.
106. Gully,D., Moinier,D., Loiseau,L. and Bouvieret,E. (2003) New partners of acyl carrier protein detected in *Escherichia coli* by tandem affinity purification. *FEBS Lett.*, **548**, 90–96.
107. Shereda,R.D., Bernstein,D.A. and Keck,J.L. (2007) A central role for SSB in *Escherichia coli* RecQ DNA helicase function. *J. Biol. Chem.*, **282**, 19247–19258.
108. Trubetskoy,D., Proux,F., Allemand,F., Dreyfus,M. and Iost,I. (2009) SrmB, a DEAD-box helicase involved in *Escherichia coli* ribosome assembly, is specifically targeted to 23S rRNA in vivo. *Nucleic Acids Res.*, **37**, 6540–6549.
109. Gupta,N. and Culver,G.M. (2014) Multiple in vivo pathways for *Escherichia coli* small ribosomal subunit assembly occur on one pre-rRNA. *Nat. Struct. Mol. Biol.*, **21**, 937–943.